Novel All-Optical On-Off Keyed to Alternate-Mark-Inversion Converter

J.M. Dailey, R.P. Webb, and R.J. Manning
Tyndall National Institute & Department of Physics, University College Cork, Lee Maltings, Cork, Ireland
james.dailey@tyndall.ie

Abstract: We numerically investigate a novel 40 Gbps OOK to AMI all-optical modulation format converter employing an SOA-based Mach-Zehnder interferometer. We demonstrate operation with a 2^7-1 PRBS and explain the phase modulation's relationship with patterning.

OCIS codes: (250.5980) Semiconductor optical amplifiers; (230.1150) All-optical devices; (060.4080) Modulation (060.5060) Phase modulation; (250.4745) Optical processing devices

1. Introduction

The ever-increasing demand for optical fiber capacity has fueled interest in advanced modulation formats enabling superior transmission properties. One such modulation format is alternate mark inversion (AMI) where on-off keyed (OOK) pulses, typically return-to-zero (RZ), are also phase modulated so that each pulse is phase-inverted with respect to the next pulse [1]. In this work we propose and numerically investigate, for the first time, the use of a semiconductor optical amplifier (SOA)-based Mach-Zehnder interferometer (MZI) for 40 Gbps all-optical modulation conversion between RZ-OOK and RZ-AMI. We also quantitatively analyze the output phase modulation through the phase compression factor.

2. Operation Principles

The SOA-based MZI is configured as an exclusive-or (XOR) logic gate [2,3], as shown in Fig. 1, with two input ports, A and B. The cw probe at λ_{AMI} is injected into the interferometer input port and propagates through the two SOAs which can change both the amplitude and phase of the probe. The upper arm of the MZI also contains a static phase shifter which controls the interference condition of the probe at the MZI output port. With no other inputs to the MZI, the two path lengths are identical, and setting the phase shifter to π leads to a destructive interference condition for the probe at the output port.

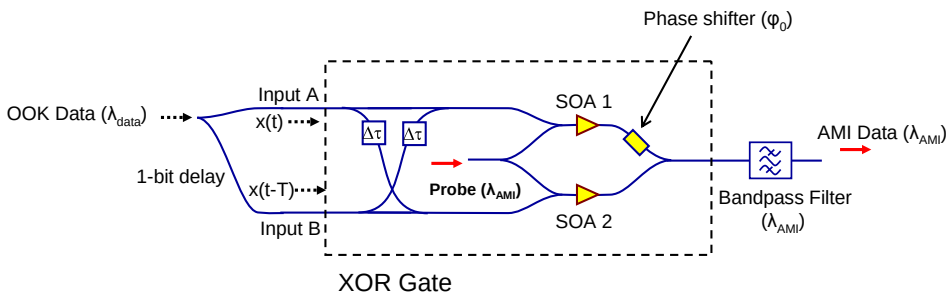

Fig. 1. All-optical modulation converter with the XOR gate shown inside dotted box.

The XOR gate is shown in the well-known push-pull configuration allowing switching windows much shorter than the SOA recovery times [2,3]. A pulse injected into input A is split between SOA1 and SOA2. The pulse first saturates SOA1, and through both cross-gain (XGM) and cross-phase modulation (XPM), the rising edge of a pulse at λ_{AMI} is created at the switch output. The other pulse is delayed and enters SOA2 $\Delta\tau$ seconds later, closing the switching window opened by SOA1, and creates the falling edge of the output pulse. Though the push-pull configuration enables the creation of short output pulses, it does not eliminate output patterning due to the finite recovery times of the SOAs.

The gate works in the same way for input B except that the SOAs are optically addressed in opposite sequence. If there is a pulse inputted to both A and B the simultaneous phase excursions in the two SOAs cancel and the switch stays closed. In this way the MZI exhibits XOR functionality, and we have recently demonstrated a 42.6 Gbps hybrid-integrated device operating with a low bit-error rate penalty [2].

To understand the phase modulation at the output we first analyze the static transfer function for the XOR gate, *H*. We consider the transfer function in the case where the delayed pull inputs and the XGM on the probe are neglected:

$$H(\phi_1,\phi_2) = e^{j\left(\frac{\pi+\phi_1+\phi_2}{2}\right)} \cdot \sin\left(\frac{\phi_2-\phi_1}{2}\right) \tag{1}$$

where φ_1 and φ_2 are the phase shifts induced on the probe by SOA1 and SOA2, respectively, and φ_0 in Fig. 1 has been set to π. *H* becomes nonzero after one of two input conditions: (1,0) and (0,1) where (A,B) are the binary inputs to ports A and B. Using Eq. (1) we can compare the two different output electric fields:

$$\frac{\vec{E}_A}{\vec{E}_B} = \frac{e^{j\left(\frac{\pi+\phi_1}{2}\right)} \cdot \sin\left(\frac{-\phi_1}{2}\right)}{e^{j\left(\frac{\pi+\phi_2}{2}\right)} \cdot \sin\left(\frac{\phi_2}{2}\right)} = \frac{-\sin\left(\frac{\phi_1}{2}\right)}{+\sin\left(\frac{\phi_1}{2}\right)} = -1 \tag{2}$$

where $\vec{E}_A$ and $\vec{E}_B$ are the electric fields resulting from (1,0) and (0,1), respectively, and we assume that φ_1 and φ_2 are equal. Eq. (2) indicates that the two possible output field states are π out of phase with each other.

We stress the important result from Eq. (2) that the phase difference between the two fields is completely independent of the magnitude of the individual phase excursions, φ_1 and φ_2. Dynamically, it is only necessary that the SOA phase excursions be equal for π phase shifts on the output pulses. This suggests that this technique will work across the SOA gain bandwidth and possess a large input dynamic range. However, we anticipate that pattern effects may cause pulse-to-pulse variations in φ_1 and φ_2 and break the necessary operational symmetry.

We demonstrate in Table 1 how injecting a copy of the data delayed by one bit period into one of the XOR input ports (port B in Fig. 1) produces AMI modulation at the output. Table 1 shows a pulse, which represents a logical "1", appearing at the output due to an input pulse ("1") at port A. This input pulse is followed by an arbitrary number of similar pulses. Each of these input pulses results in a no-pulse, or logical zero, at the XOR output due to the delayed copy injected into port B. When a logical zero eventually enters port A, the pulse injected into port B creates an output pulse which must be of opposite phase as shown in Eq. (2). Similarly, Table 2 shows how a sequence of zeros also results in output pulses of alternating phase. We note that the AMI pulse sequence outputted from the gate is not identical to the input binary logic sequence, but this difference can be removed using a simple encoder/decoder which can in principle be implemented either electronically or all-optically.

Table 1

A	1	1	…	1	0
B	0	1	…	1	1
Output	-1	0	…	0	+1

Table 2

A	0	0	…	0	1
B	1	0	…	0	0
Output	+1	0	…	0	-1

3. Modeling

We now investigate the operation of the complete all-optical modulation converter shown in Fig. 1 using a computer model based on a typical traveling-wave rate-equation analysis [4]. Typical modeling parameters [4] are utilized, resulting in SOAs which are 2mm in length and when biased at 350 mA produce a gain peak of 30 dB centered at 1548 nm. The gain recovery time is ~ 22 ps which suggests that these SOAs will perform well for input data sequences at 40 Gbps. However, we expect patterning to persist at the output because each SOA is receiving both push and pull (i.e. delayed by $\Delta\tau$) inputs.

The cw probe and data wavelengths are 1549.32 nm and 1548.51 nm, respectively. The probe input power into the modulation converter is -7 dBm. The 40 Gbps OOK data is composed of 3 ps optical pulses with an average power of -4.2 dBm (2.8 mW peak power) which are modulated with a 2^7-1 pseudo-random binary sequence (PRBS). The delay built into the pull optical path is 8 ps, and the static phase shifter is set to π.

The two input signals injected into ports A and B at λ_{data}, as well as the output signal at λ_{AMI}, are shown in Fig. 2. The plot shows power as a function of time in units of bit number. Input B (middle trace) is clearly delayed from input A (top trace) by one bit period. The entire output electric field trace is multiplied by a single constant to minimize the imaginary components, and the bottom trace in Fig. 2 shows the output power multiplied by the sign of the real part of the output field. This trace depicts the pulse to pulse phase reversals as sign changes which are seen to be consistent with AMI modulation.

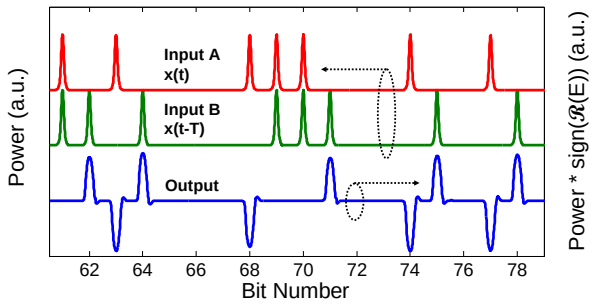

Fig. 2. Input and output pulses from the modulation converter.

We expect finite SOA recovery times to lead to both amplitude and phase patterning on the output. Furthermore, we anticipate that patterning may lead to an overall mean pulse-to-pulse phase shift which is not equal to π (see Eq. (2)). The output electric field is sampled in each bit slot and displayed as a point in the constellation diagram in Fig. 3a. We take the average vector angle of each of the mark subsets as φ_{+1} ($\Re\{E\}>0$) and φ_{-1} ($\Re\{E\}<0$) and define the phase compression, Δφ,

$$\Delta\phi \equiv 1 - \frac{|\phi_{+1} - \phi_{-1}|}{\pi} \tag{3}$$

and offer Δφ as a metric for the efficacy of the modulation converter. The model predicts a phase compression of 9% for this modulation converter operating at 40 Gbps. The source of the phase compression lies in the finite SOA recovery time. On every occurrence of input condition (0,1), a pulse must have *necessarily* been inputted to port A in the immediately preceding bit period. This means that the switch can never be in a completely recovered state on input condition (0,1), and the resultant output pulses will have less of an average phase shift than their counterparts for input condition (1,0). The result is a mean phase angle between the output pulses which is not equal to π radians.

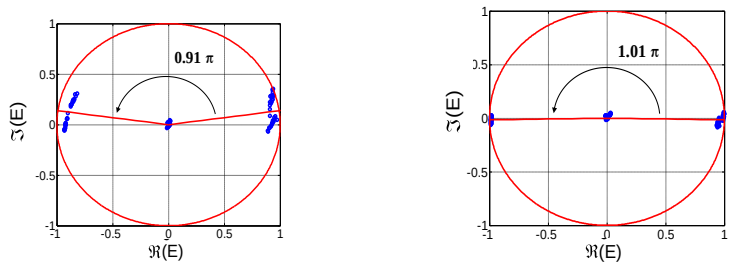

(a) (b)

Fig. 3. (a) Constellation diagram of the 40 Gbps output. (b) Constellation for 20 Gbps output.

This suggests that allowing more time for the SOAs to recover will decrease the phase compression. We repeat the previous numerical experiment with identical parameters except for a longer bit period of 50ps. The results are shown in Fig. 3b, where the constellation clearly demonstrates less amplitude and phase patterning as well as a much smaller phase compression.

4. Conclusion

We have proposed and analyzed a novel high-speed all-optical OOK to AMI modulation converter, which is a function of interest in future optical networks. The device's reliance on MZI symmetry suggests generous tolerances to input pulse width, power, and wavelength. We also show that scaling to higher bitrates is limited by phase compression and patterning.

Acknowledgment: This work was supported by Science Foundation Ireland under grant 06/IN/I969.

5. References

[1] P.J. Winzer, et al,"40-Gb/s Return-to-Zero Alternate-Mark-Inversion (RZ-AMI) Transmission Over 2000 km," IEEE PTL **15**, 766-68 (2003).
[2] J.M. Dailey, et al, **"**42.6 Gbit/s fully integrated all-optical XOR gate," Electron. Lett **45**, 1047-49 (2009).
[3] R.P. Webb, et al, "40 Gbit/s all-optical XOR gate based on hybrid-integrated Mach-Zehnder interferometer," Electron. Lett **39**, 79-81 (2003).
[4] J.M. Dailey, et al, "Simple Design Rules for Optimizing Asymmetries in SOA-Based Mach-Zehnder Wavelength Converters," IEEE JLT **27**, 1480-88 (2009).